Clim Dyn (2007) 29:633–645
DOI 10.1007/s00382-007-0253-x

Teleconnection patterns and Rossby wave propagation associated to generalized frosts over southern South America

Gabriela V. Müller · Tércio Ambrizzi

Received: 12 July 2006 / Accepted: 22 March 2007 / Published online: 27 April 2007

Abstract Based on previous observational studies of the mean atmospheric circulation leading to generalized frosts (GF) in central Southern South America, it is possible to establish a hypothesis that specific large scale patterns are associated to the frequency of occurrence of these events through the propagation of Rossby waves remotely excited. This hypothesis is tested here through a teleconnection analysis for austral winters which present an extreme frequency of occurrence of GF in southeastern South America, particularly over the Wet Pampa area in Argentina. Rossby wave propagation regions are identified for two basic states given by the composition of winters with maximum and minimum frequency of GF occurrence, during the 1961–1990 period. The stationary wavenumber K_s indicates the regions where the Rossby wave propagation is permitted and those where it will be inhibited ($K_s = 0$), highlighting the importance of the jets as waveguides. Nevertheless, differences exist between both basic states analyzed. These differences indicate that the locations for wave generation and its later evolution are conditioned by the basic state. Results are validated through a baroclinic model, which simulates the Rossby wave patterns responsible for the teleconnection. Numerical experiments confirm that the principal wave activity takes place inside the subtropical and polar jets. In particular, for the basic state with maximum frequency of GF occurrence, the wave trains propagating inside the subtropical and polar waveguides merge just before entering the continent, as shown by the observations prior to the occurrence of GF events. This configuration favors the development of an intense south wind anomaly with large meridional extension which results in the intensification of anticyclonic circulation in southern South America. A conceptual model is presented to summarise all these results.

G. V. Müller (✉) · T. Ambrizzi
Institute of Astronomy, Geophysics and Atmospheric Sciences, University of São Paulo, Rua do Matão 1226, São Paulo, Brazil
e-mail: gabriela@model.iag.usp.br

T. Ambrizzi
e-mail: ambrizzi@model.iag.usp.br

1 Introduction

The identification of teleconnection patterns and the analysis of their effect on the horizontal structure of the atmospheric circulation can be very useful to understand anomalous events in many regions of the world. Local forcing in specific places can influence remote regions through organized structures in form of waves. One way to analyze this wave propagation is using the stationary Rossby wave linear theory in a barotropic atmosphere. Previous studies on atmospheric teleconnection patterns have shown that linear wave theory may explain some of the observed low-frequency variability (e.g. Hoskins and Karoly 1981). Using a climatological December–January–February (DJF) basic flow and a simple barotropic model, Hoskins and Ambrizzi (1993) examined the preferred trajectories followed by Rossby waves around the globe. For instance, through the analysis of climatological stationary wavenumber fields (K_s) they found that the upper level tropospheric jets can act as waveguides in the atmosphere. In particular, during the Southern Hemisphere winter (June–July–August, JJA), Ambrizzi et al. (1995) have numerically demonstrated using a barotropic model that the subtropical and polar jets have such characteristic. Using a multi-level primitive equation model, Ambrizzi and

Hoskins (1997) indicate that the essential characteristics obtained by the barotropic analysis of the Rossby wave propagation over the sphere are also valid for a three dimensional basic state. The authors suggest that the atmospheric dynamics at large scales can be qualitatively interpreted through the linear wave theory.

The importance of the jets as waveguides has also been observed by Berbery and Vera (1996) who have shown that synoptic-scale waves propagate over the South Pacific Ocean along two main paths. This is also evident in the propagation of the wave trains which reach South America and can cause a severe drop of surface temperature and therefore are responsible for frost in large parts of the South American continent (Müller et al. 2005). Through an atmospheric circulation analysis during generalized frost (GF) events in central southern South America, Müller et al. (2005) showed that for the winter with maximum frequency of GF occurrence in the Argentinean Wet Pampas (Pampa Húmeda) the wave trains propagation along the Pacific coincide with the position of the subtropical and polar jets. An interesting feature of these wave trains is their phase coincidence just before they reach South America. This condition is only present prior to a GF event as shown in Fig. 1, adapted from Müller et al. (2005). It is seen in the figure that this configuration favors the development of an intense southerly wind anomaly with large meridional extension that intensifies the anticyclonic circulation over its area of influence and contributes to a marked meridional polar air outbreak into the continent. In particular in the day 0 (Fig. 1d), there is anomalous southerly flow over the study region, so that the cold and dry air favors the frost development over the Wet Pampa.

In general the relationship between wave propagation patterns and cold outbreaks over South America found in the literature was always associated to the existence of one wavetrain (e.g., Marengo et al. 1997; Cavalcanti and Kayano 1999; Vera and Vigliarolo 2000). In particular the less persistent GF events, recently studied by Müller and Berri (2007) also show this feature, i.e. an arc-shaped wave train that starts in the central-eastern Pacific Ocean and propagates across the midlatitudes of the Southern Hemisphere, initially poleward and then curved towards the Equator. Upon reaching the continent, the wave train continues to propagate of the NE affecting all the southern cone of South America. However, a double wavetrain seems to be a characteristic of more persistent GF events (Müller and Berri 2007) as well as of more frequent GF events, as shown by the results of Müller et al. (2005). These characteristics are not only seen in the composite of the observed GF events but also in the individual cases, for example the one shown in Müller and Berri (2007) in which the double wave train is clearly seen (Fig. 15 of this last paper). Therefore, the most ''conspicuous'' GF events are associated to a double wave train with phases which coincide prior to the occurrence of such events to the west of the South American continent.

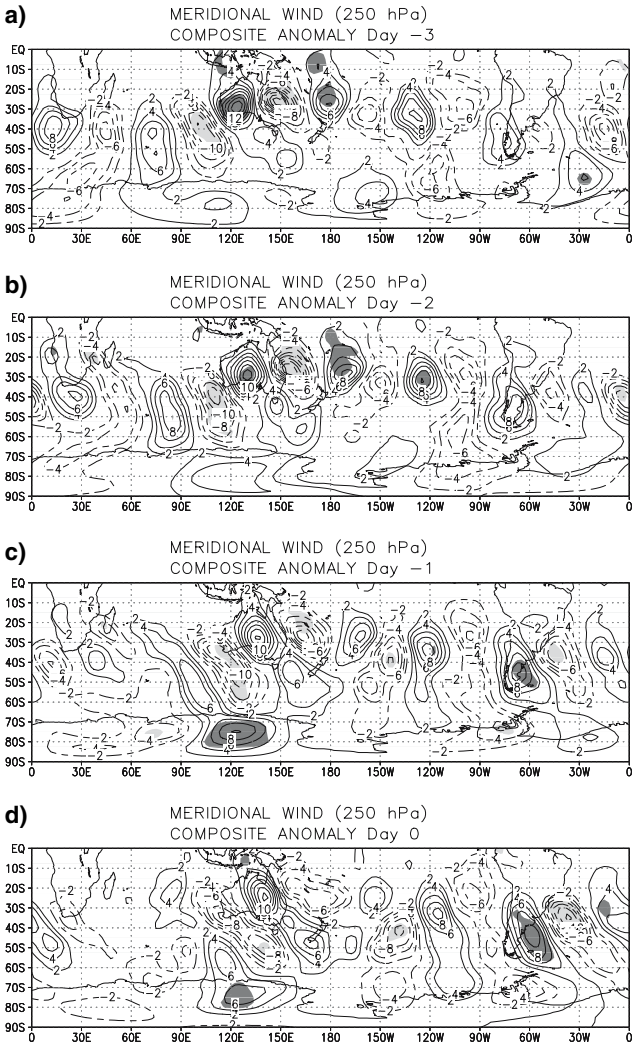

Fig. 1 Composites of meridional wind anomaly fields from day –3 to day 0 at 250 hPa (**a**–**d**) for GF events in the winters of maximum frequency of occurrence. Positive (negative) contours is in *full* (*dotted*) line at 2 ms^{-1} intervals. The *shaded areas* are significant at the 99% level according to the Student's *t*-test (adapted from Müller et al. 2005)

As mentioned by Hoskins (1983), teleconnection studies are a good example of the relationship between observations theory and models. Using the linear wave theory and numerical experiments with a baroclinic model, this study will analyze the dynamical conditions for the wave phase coincidence prior to the occurrence of GF over the central-southern South America. For that purpose the winters with extreme GF frequency are selected and analyzed. Section 2.1 provides a brief description of the criterion and the data used for this selection. Based on the linear wave

theory, described in Sect. 2.2, we present in Sect. 3.1 an analysis of the main characteristics of the atmospheric basic flow during the winters with extreme GF frequency: maximum and minimum frequency of GF occurrence. In particular, the physical aspects revealed by the basic state with maximum frequency of GF are employed to define the numerical experiments presented in Sect. 3.2. The multi-level primitive equation model used for these simulations is briefly described in Sect. 2.3.

All these elements—observational and numerical results and theorical aspect—are used to visualize a conceptual model of the teleconnection patterns in order to explain the atmospheric physical mechanisms responsible for GF occurrence during the austral winters with maximum frequency of such events. In the Sect. 4 is presented the conceptual model and the summary of the main results and conclusions is given in Sect. 5.

2 Data and methodology

2.1 Data and criterion for the selected generalized frosts events

Following Müller et al. (2000), the spatial criterion used to select GF events is defined as days on which surface temperature below 0°C is recorded at more than 75% of the meteorological stations in the wet Pampas in Argentina, a domain defined between 27°, 40°S and 65°, 57°W (details on the selection of frosts and their position can be found in Müller 2006). This region is an extended plain of over 750,000 km^2 with a very important agriculture production. The GF events have a spatial representativeness which, in principle, would make the sample homogeneous and specifically independent from the intensity of regularly cold waves that affect the region, its latitudinal penetration or its persistence (Müller et al. 2005).

Müller et al. (2000) and Müller (2006) showed that there is a great interannual and interseasonal variability of frosts in the central-east part of southern South America. Therefore, to understand the large scale atmospheric circulation associated with these cold episodes, Müller et al. (2005) isolated those years of extreme frequency of frost occurrence. A maximum (minimum) frequency of GF occurrence is considered when frosts are one standard deviation (σ) above (below) the mean values during the austral winter (JJA) for the period 1961–1990 (GF $+\sigma$ and GF $-\sigma$, respectively). The analysis of the atmospheric basic flow in the following sections will be based on the composites of the GF $+\sigma$ and GF $-\sigma$ winters. The NCEP reanalysis data with a horizontal resolution of 2.5° of latitude and longitude are used in the analysis.

The years and the number of the GF occurrences above (GF $+\sigma$) or below (GF $-\sigma$) one standard deviation from the average number of events are shown in Table 1. It is interesting to notice that there can be as much as 14 GF events in 1 year or none in others. The composition of these individual events (see Müller et al. 2005, for a detailed description of the selection criteria) is shown in Fig. 1.

2.2 Stationary wavenumber

According to Kiladis (1998) a useful diagnostic tool to represent the mean background state in which the transients are embedded is the calculation of the stationary Rossby wavenumber which is given by $K_S = (\beta*/\bar{U})^{1/2}$ where $\beta^* = \beta - \partial^2\bar{U}/\partial y^2$is the meridional gradient of absolute vorticity associated with the basic state and K_s is the total wavenumber at which a barotropic Rossby wave is stationary at a particular location in a given background zonal flow ($\bar{U}$). Hoskins and Ambrizzi (1993) and others showed that the distribution of K_s can be used to infer the location of critical lines and waveguides for stationary Rossby waves. For example, zonally oriented regions of relative high values of K_s bounded by lower values to the north and south (usually associated with strong jet streams) indicate sectors favorable for guiding Rossby waves. Although the waves studied here are clearly not stationary, Yang and Hoskins (1996) show that a modified K (total wavenumber) for transient waves can still give useful information on the dependence of nonstationary eddy activity on the background state. Here we will use K_s to give a qualitative picture of the effects of the basic state flow within the westerly duct on the subtropical and polar wave propagation and a first assessment of the impact of the GF basic flow on the dynamical structure relevant for the Rossby wave dispersion.

2.3 Baroclinic model

In order to test the generation of extratropical wave patterns which favor the development of extreme cold

Table 1 Years of maximum ($+\sigma$) and minimum ($-\sigma$) frequency of GF occurrence and number of events

	JJA	*N*
$+\sigma$	1970	11
	1976	14
	1988	13
$-\sigma$	1968	1
	1973	0
	1982	2
	1986	0

events over the southeast of South America, numerical simulations using a primitive equation model were carried out. The baroclinic model used in the present study was originally developed by Hoskins and Simmons (1975), and extensively used in the study of large scale circulations forced by convective sources (e.g., Ambrizzi and Hoskins 1997; Cavalcanti 2000; Marengo et al. 2002). Although the model is dry and do not include any physical process linked to the phase change of water vapor, many aspects of the atmosphere dynamics can be reproduced from synoptic scale systems (Hoskins and Simmons 1975) to large scale perturbations (Valdes and Hoskins 1989). The model has a global domain, is spectrally truncated with a total zonal wavenumber 42 (T42) and it has 12 vertical sigma levels. It also includes horizontal and vertical diffusion and Newtonian cooling (see Jin and Hoskins 1995, for details). For initial condition it uses geopotential height, zonal and meridional wind and temperature. Further details of the model will be given in Sect. 3.

3 Results

3.1 Basic state during winters with extreme GF frequency

Rossby waves propagation depends on the basic state in which they propagate and on the source generating these waves (Ambrizzi et al. 1995). Therefore, the basic state which represents winters with highest frequency of GF occurrence, i.e. $+\sigma$, must have particular characteristics which favor the formation of GF. In an analogous way, winters with minimum frequency of GF occurrence, i.e. $-\sigma$, must present conditions which do not favor the formation of GF. Consequently, in this section, both basic states, $+\sigma$ *y* $-\sigma$, will be studied following the linear Rossby wave theory.

The main basic state features for $+\sigma$ and $-\sigma$ are depicted in Fig. 2. Figure 2a ($+\sigma$ winters) shows the mean zonal wind at 250 hPa where the maximum values are around 30°S extending from the Indian Ocean to the Pacific

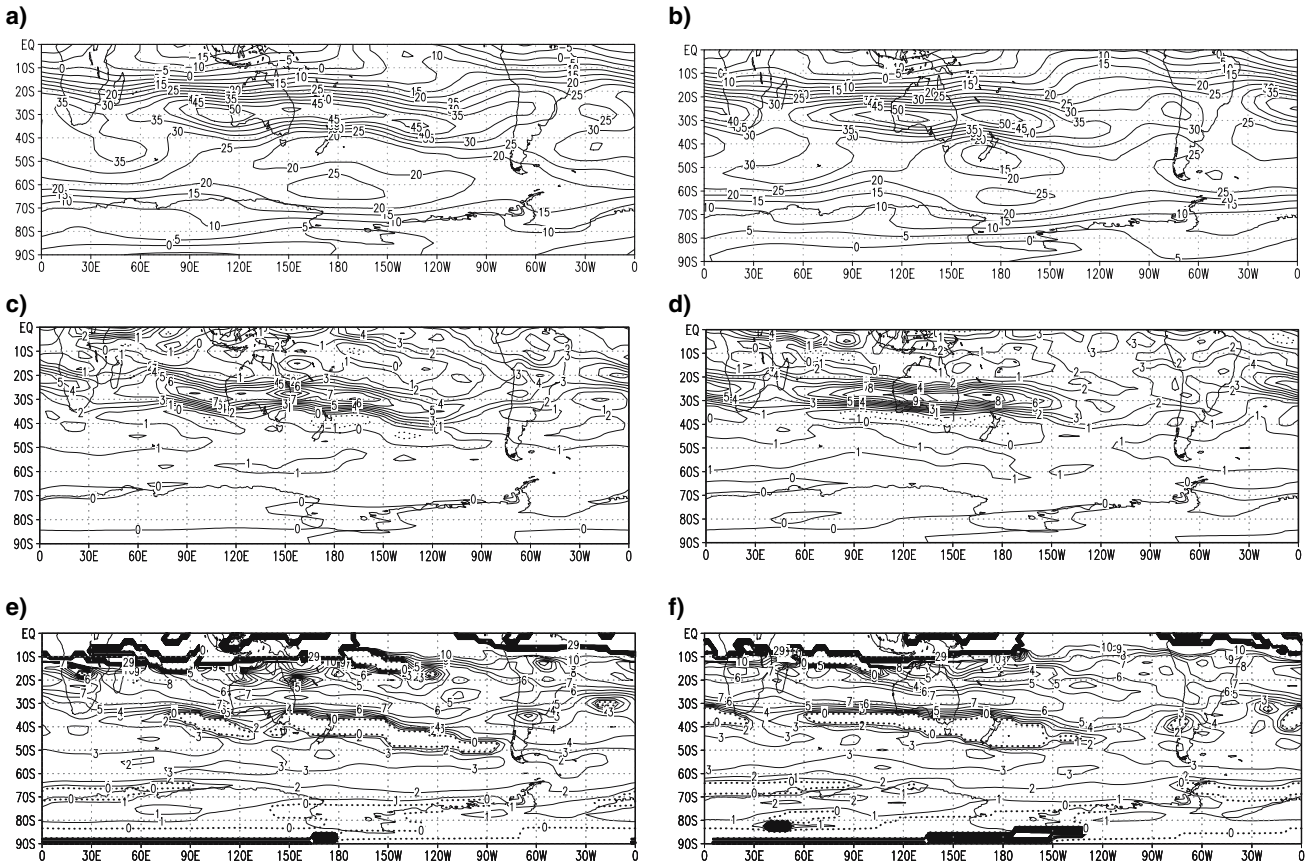

Fig. 2 Zonal wind component at 250 hPa (*continuos lines*, ms^{-1}) for the austral winters $+\sigma$ (**a**) and $-\sigma$ (**b**) composities; meridional gradient of absolute vorticity (β_M) in mercator coordinates at 250 hPa, for the austral winters $+\sigma$ (**c**) and $-\sigma$ (**d**), where *dotted lines* indicate negative values and lines are drawn every 1×10^{-11} s^{-1} m^{-1}. Stationary wavenumber K_s at 250 hPa corresponding to $+\sigma$ (**e**) and $-\sigma$ (**f**) austral winters, where *thick contours* indicate singular values and *dotted lines* represent $K_s = 0$

Ocean. The core maximum is around 50 ms^{-1} and it is located in the eastern Indian Ocean, being displaced 60° to the west of the climatological reference mean (winter JJA 1961–1990). The 35 ms^{-1} isotach reaches the South American continent with a second nucleus which extends southeastwards from southern South Africa. An outstanding characteristic is the zonal wind gradient in the region of the southwestern Indian Ocean. At high latitudes the zonal wind maxima, between 20 and 25 ms^{-1}, are located along the 60°S; the polar jet position is also different from that of the climatology with a ''tongue'' towards South America with a longitudinal extension closer to the continent. Fig. 2b ($-\sigma$ winters) shows a subtropical jet divided in two zones, one from the Atlantic Ocean up to South Africa and other from the Indian Ocean until the central Pacific. The subtropical jet has two maxima in this case, one centred around 30°S to the southwest of Australia and the other at approximately 180° longitude. South of the latter, just on the date line, there is a secondary zonal wind maximum.

The region where the jet exhibits its highest values is where the meridional gradient of absolute vorticity reaches its maximum, with minima to the north and south of the jet. Figure 2c, d show the meridional gradient of absolute vorticity which is drawn in Mercator coordinates (β_M as in Hoskins and Ambrizzi 1993). It can be seen that the maximum gradients of β_M coincide with the zonal wind maximum regions (Fig. 2a, b); while the minimum gradients, with zero and even negative values, are found in the polar and equatorial sides of the subtropical jet.

The geographic distribution of the stationary wave number (K_s) defined in Sect. 2.2 is shown in Fig. 2e, f. The zero wind contours ($\bar{U} = 0$) are presented in bold in the figure while those corresponding to zero K_s (i.e. $\beta_M = 0$) in a dotted line. The equatorial belt is dominated by a sector where the propagation is inhibited due to the presence of a transition from westerly to easterly flow, which forms a ''critical line'' to the propagation of stationary Rossby waves. This region is marked with thicker lines in Fig. 2e, f indicating high wave number values ($K_s \geq 20$). A local maximum of K_s in the region of maximum zonal winds, i.e. along the subtropical jet, show wave numbers 6 and 7 in both winter groups. This region also contains uniform values of K_s meridionaly limited by smaller ones.

In the polar side of the subtropical jet the presence of $K_s = 0$ inhibits the propagation of Rossby waves through it, because according to the wave theory, they must deviate before reaching this region. There the $K_s = 0$ line can act as a waveguide boundary. An interesting feature in this last case is the difference in the longitudinal extension of K_s for $+\sigma$ (Fig. 2e) with respect to $-\sigma$ (Fig. 2f). In the first map this region extends very near to the South American continent. However, the K_s pattern for the $-\sigma$ winters (Fig. 2f) shows a shorter extension of the waveguide duct, besides of a region of zero K_s between 35 and 40°S in the west of Argentina which coincides with the main entrance region of weather systems over South America (Garreaud 2000; Seluchi and Marengo 2000, among others). This feature is not seen in the $+\sigma$ case and it may have some influence on the Rossby wave propagation path and, therefore, in the events analyzed.

In order to better visualize the characteristics of K_s in the $+\sigma$ and $-\sigma$ winters, meridional profiles at different longitudes are shown in Fig. 3. The first profiles were positioned in the region of entrance of synoptic systems over the South American continent, which are important to frost events, and is centered at 85°W (Fig. 3a). In the right panel, corresponding to $-\sigma$, a discontinuous curve with zero value of K_s between 35 and 40°S approximately is observed. Compared to $+\sigma$ (left panel), the meridional profile of K_s decreases towards higher latitudes with peak with wave numbers between 3 and 4 around 40°S, in the latitudes where $-\sigma$ presents null values (Fig. 3b). This local maximum acts as a weak wave guide. So, while Rossby waves in the $+\sigma$ cases can propagate in the region, they will be inhibited in the case of $-\sigma$ basic state. The other selected longitudes for the K_s analysis (Fig. 2e, f) are: 110°W, which refers to the exit region of the subtropical jet; 170°E and 120°E which coincide with the maximum intensity of the polar and the subtropical jets; and finally 45°E which is related to the secondary maximum of the zonal wind component of $+\sigma$ to the southeast of South Africa (see Fig. 2a). When looking at the K_s profiles (Fig. 3b–e), basically two bands of latitudes present the maximum values in the $+\sigma$ (left panel) and $-\sigma$ (right panel) winters. They correspond to the latitudes of the polar and subtropical jets. These regions act as waveguides for the Rossby waves (e.g., Berbery et al. 1992; Ambrizzi et al. 1995; Ambrizzi and Hoskins 1997). The wave propagation in the subtropical jet has shorter wavelengths with numbers 6 and 7. On the other hand, longer wavelengths are observed in the polar jet with wavenumbers around 3 and 4 (Fig. 3c, d). Moreover, the K_s profiles for higher latitudes present values gradually reaching zero, coinciding with the results obtained by Karoly (1983) for a climatological austral winter basic state.

Based on Fig. 3, some hypothesis arise from the analysis of the possible trajectories that can be followed by the different waves in each basic state, $+\sigma$ and $-\sigma$. Along the Pacific Ocean (Fig. 3c, d) waves will clearly be trapped by the subtropical and polar jets, where the maximum in K_s is flanked by minima values. Over the Indian Ocean (Fig. 3e), the wave trapping is less intense, though one can still see the presence of two waveguides. However, the most important differences in the K_s meridional profiles occur near the South American continent, between 85 and 110°W (Fig. 3a, b, respectively). Just before waves can reach the

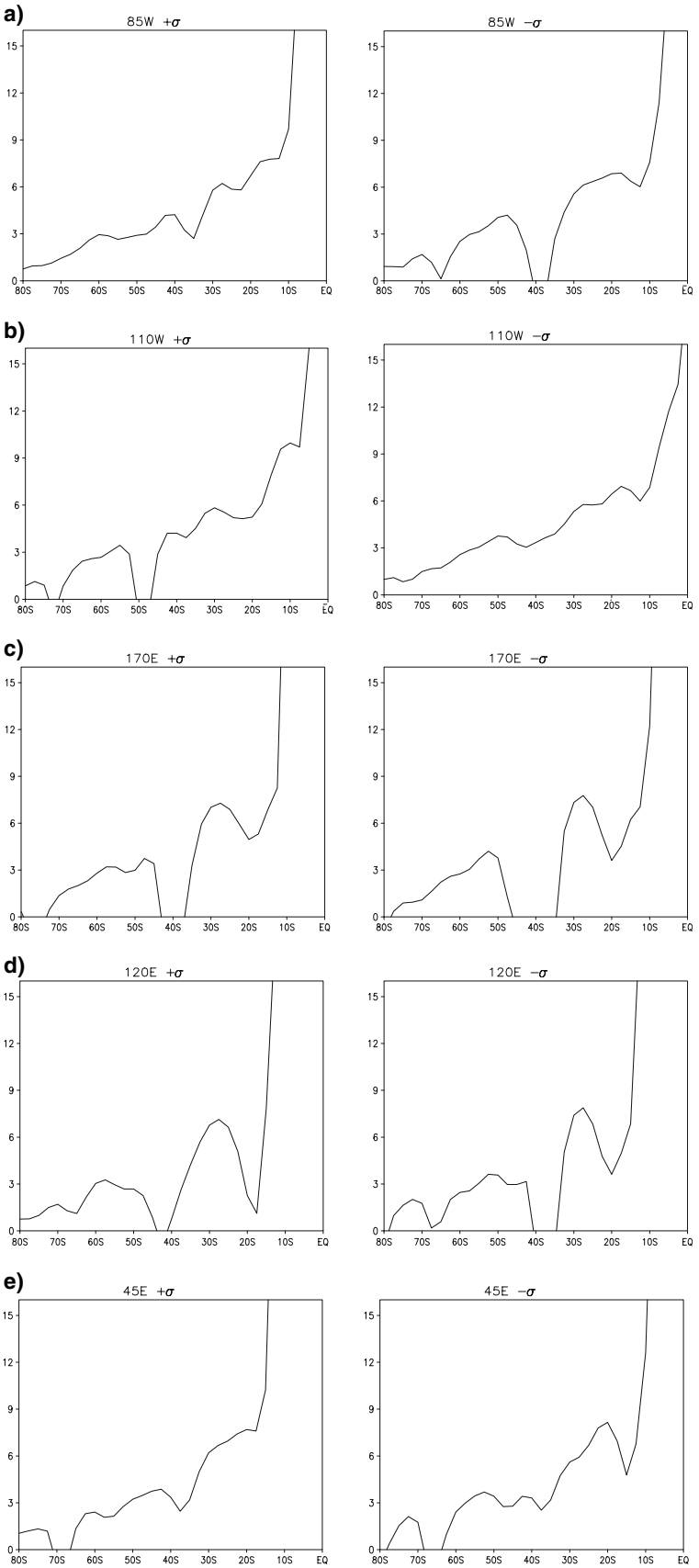

Fig. 3 Stationary wavenumber (K_s) meridional profiles at 85°W (**a**), 110°W (**b**), 170°E (**c**), 120°E (**d**) and 45°E (**e**) corresponding to $+\sigma$ (*left panel*) and $-\sigma$ (*right panel*) austral winters

continent, the waveguide for the $+\sigma$ basic state is well defined, with two peaks of K_s separating the subtropical and polar waves. However, over the continent (Fig. 3a, left panel), one cannot see any clear separation which means that the waves may interact with each other. A reverse pattern is observed for the $-\sigma$ basic state. The waveguide near the continent (Fig. 3b, right panel) is not too intense and the subtropical and polar waves are free to propagate in this region. However, over the continent (Fig. 3a, right panel), there is a clear separation of propagation paths, which suggest that wave interaction in the South of South America is more difficult.

All the elements mentioned above support the basic hypothesis of this study, that is, the occurrence of extreme cold events in the Wet Pampa, Argentina, is influenced by large scale atmospheric circulation patterns. In particular, depending on the basic state where the Rossby waves are propagating and therefore the position of the atmospheric waveguides, there can be an interaction between subtropical and polar waves over the South American continent and the generation of a right environment for the occurrence of a GF in the Wet Pampa.

Based on the observational results obtained by Müller et al. (2005) and the linear wave theory discussed so far, using the atmospheric basic state composites for winters with maximum and minimum frequency of GF, next section will present some results from numerical simulations produced by a simple baroclinic model. The focus of the experiments is to determine physical mechanisms intervening in the large scale dynamics which leads to extreme cold events causing the GF events.

3.2 Modeling experiments

In this section, we describe simple baroclinic modeling experiments that were performed in order to verify the large scale atmospheric patterns responsible for the GF events, in particular, the interaction of the Rossby waves propagating through the subtropical and polar waveguides. The model uses a thermal forcing with a horizontal elliptic structure and fixed position (latitude and longitude) to perturb the atmosphere. The heating has a vertical profile with the amplitude following a cosine function, with a maximum at 400 hPa level, corresponding to a 5°C day^{-1}. The role of the heat source is solely to excite the Rossby waves, acting as a *wave maker*, and it is associated to mean atmospheric conditions arising from the linear analysis of the $+\sigma$ basic state (see Sect. 3.1).

The model was integrated for 14 days being enough to acquire a stationary pattern. The anomaly patterns to be shown from the numerical results are obtained from the difference between the day 14 of integration and day 0, which represent the basic state before the heating forcing is initiated. More details about the model can be found in Ambrizzi and Hoskins (1997) and references therein.

3.2.1 *Basic state of maximum GF frequency ($+\sigma$)*

Section 3.1 showed that the $+\sigma$ basic state contains the subtropical and polar jets and that they can act as waveguides. In particular the presence of the polar jet seems to play a relevant role in the waves reaching South America during winters. Taken these aspects into consideration the forcing in the first experiment was positioned at 45°E, 40°S. The position of this forcing is first chosen in a region with a relative maximum in the zonal wind for the $+\sigma$ basic state (see Fig. 2a). It is situated approximately downstream of the area where the zonal wave number (K_s) is zero (see Fig. 2e), i.e. where the meridional absolute vorticity gradient (β_M) is zero or negative (see Fig. 2c).

Similar experiment by using a basic state composed by winters—May to September—of the Southern Hemisphere (1980–1985), was done by Berbery et al. (1992) who identified a reflective zone (i.e. with negative absolute vorticity meridional gradient) south of the subtropical jet, which acts as deflector of the wave energy from that region. Through observations and numerical simulations they showed that the wave train to the southwest of Australia is divided and guided by the subtropical and polar jets towards the east. A similar result was found for a $+\sigma$ basic state simulation for the source at 45°E, 40°S as depicted in Fig. 4. This forcing generates a wave train which splits in two and propagates along the respective jets following basically a zonal trajectory. Although the trajectories along both jets acquire certain anticyclonic curvature in the central Pacific, they do not join in the southeast Pacific, reaching the South American continent separately. The positive meridional wind anomaly only affects the southern cone of Argentina (see Fig. 4).

From the comparison between Figs. 4 and 1, it is clear that the simulated wave pattern does not agree with the observational analysis found by Müller et al. (2005). There is some suggestion that the energy propagating inside the

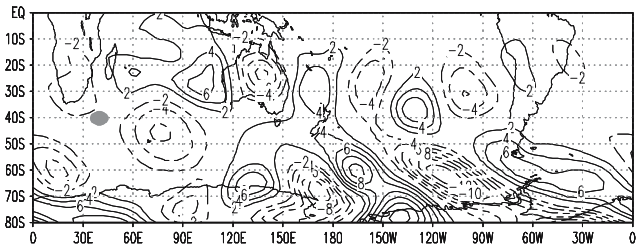

Fig. 4 Meridional wind component anomalies (ms^{-1}) at 250 hPa for day 14 of integration, corresponding to the simulation of $+\sigma$ basic state with a forcing at 45°E, 40°S (see *black dot* in the figure). Contour interval is 2 ms^{-1}

waveguides was not strong enough to generate the right environment for the GF event. Hence, another heating source is added to the experiment in order to verify the hypothesis. The position of the new forcing is closed to the subtropical jet entrance in the tropical Indian Ocean (see Fig. 2a), upstream of the principal zonal wind maximum, i.e., at 40°E, 20°S. Ambrizzi et al. (1995) in an observational and numerical analysis on teleconection patterns for a basic state composed of austral winters, demonstrate that this region in particular presents a strong teleconnection with South America, where a perturbation in this region generates Rossby waves that propagates along the subtropical jet in the Pacific Ocean until it reaches South America. This result is also in agreement with the lag correlation analysis performed by them, who concluded that regions with strong teleconnectivity tend to be oriented in the zonal direction coinciding with the position of the principal jet. Moreover, the patterns they simulated are in good agreement with the results of the teleconnectivity analysis. These results motivated the election of the point 40°E, 20°S as the position for the addicional forcing. Thus, the following experiment considers two forcings in the south Indian Ocean, one at the entrance of the principal zonal wind maximum (40°E, 20°S) and the other situated in a secondary zonal wind maximum (45°E, 40°S), both observed during $+\sigma$ winters (see Fig. 2a).

Figure 5a shows the meridional wind anomalies at 250 hPa, and depicts a wave train at approximately 30°S propagating from the central Indian Ocean across the Pacific Ocean, guided by the subtropical jet. In subpolar latitudes, another wave train propagates across the south Pacific towards the Atlantic Ocean. Their phases coincide in the Pacific eastern sector, being remarkable the meridional extension of the anomalies over the Andes. In the observational analysis of $+\sigma$ winters daily composites of GF events presented in Fig. 1, it is possible to observe the evolution of wave trains propagating along jets that, previous to GF events, their phase coincide before entering the continent (Fig. 1a, b). From this moment onwards the wave intensifies and continues to evolve propagating northeastward. The configuration of the anomaly patterns simulated by the baroclinic model is very similar to the observed one, not only at upper levels but also in the lower levels (Fig. 5b). However, a closer look to this pattern indicates that the stationary response of the model is similar to Day –2 (Fig. 1b) rather than the Day 0 of the observational pattern associated with frost (Fig. 1d). It is possible that a favorable environment in terms of basic state may be formed before the occurrence of the frost event, meaning that the position of the waveguides to generate the wave phase coincidence happens a couple of days before the GF. In fact, the stationary response of the model only suggests that given a proper basic state, the perturbed wave propagation will generate an atmospheric circulation close to South America that may favor the GF events. The interaction between the low frequency and the transients is a more complex matter which is currently been investigated and it can not be solved by the simple baroclinic model used in this study.

Based on the K_s field (Fig. 2e), the trajectory followed by the waves was already expected. As it was discussed, the separation between the subtropical and polar waveguides ends before the south cone of South America. On the other hand, over the continent, around 35°S, 70°W, there is a K_s minimum zone, which forces the waves coming from the subtropical region turning to the north and south (see Fig. 5a). This is due to one of the most important implications of the Rossby wave linear theory, they separate from regions where the basic flow determines low stationary wave numbers (K_s).

In fact, this configuration is consistent with Fig. 2e where to the north of the minimum K_s, there are discrete local maximum centres of K_s to the east of 90°W and this maximum belt has K_s = 6–8, larger than the south maximum belt around 40–45°S which has K_s = 4. It seems that the subtropical wave train splits into two when it meets the K_s minimum zone, with smaller (larger) scale wave activity propagating to north (south) and the later being crucial for

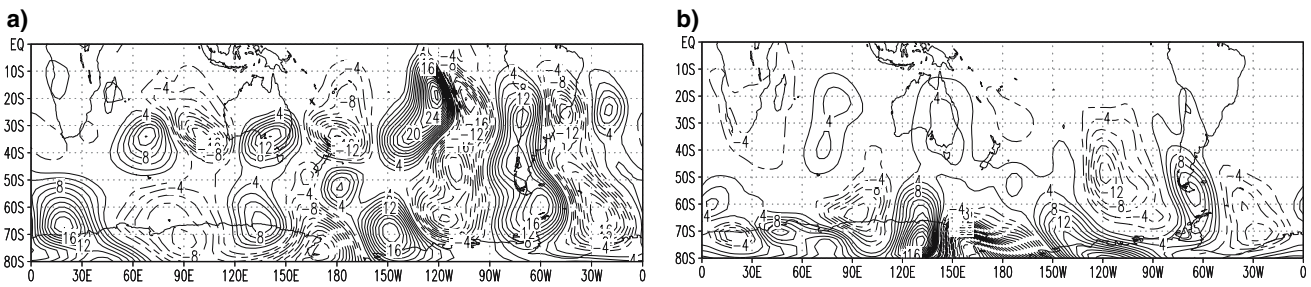

Fig. 5 Meridional wind component anomalies (ms^{-1}) at 250 hPa (**a**) and at 850 hPa (**b**) for day 14 of integration, corresponding to the simulation of $+\sigma$ basic state with two forcings: at 40°E, 20°S and 45°E, 40°S. Contour interval ia 2 ms^{-1}

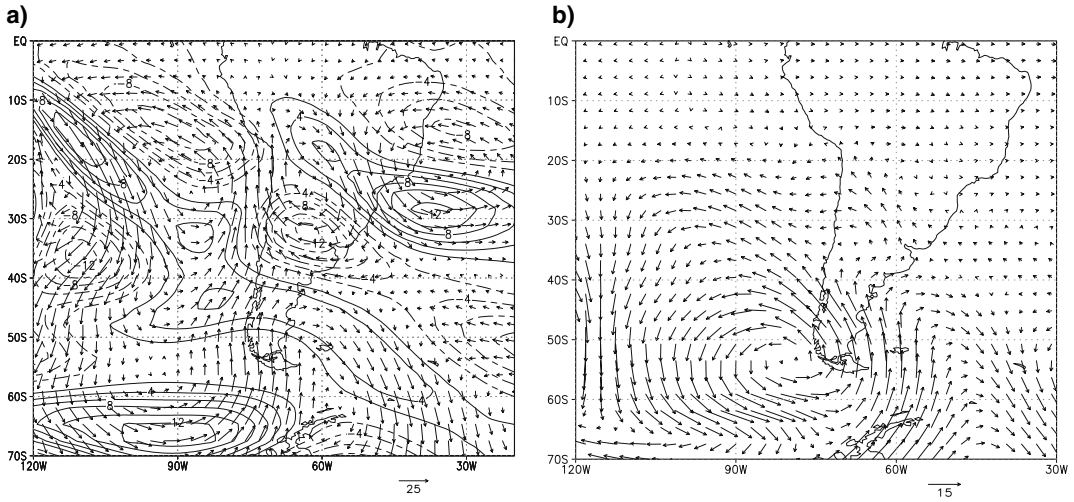

Fig. 6 Wind vector anomalies (ms^{-1}) at 250 hPa (**a**) and 850 hPa (**b**) for day 14 of integration, corresponding to the numerical simulation depicted in Fig. 5. Contours of zonal wind anomalies are also shown in **a** with interval of 2 ms^{-1}

$+\sigma$ events when it meets the polar wave. This configuration creates the right environment for the wave phase coincidence over the south of South America.

The phase coincidence is important because it favors the polar air advection over the southern part of the continent which generates the conditions for a continuous drop of surface temperature over an extended region. This feature is fundamental in the development of the GF and it is observed in the simulated wind anomalies depicted in Fig. 6. In fact, this figure is similar to the observed $+\sigma$ GF composites showed by Müller et al. (2005, see their Fig. 10). Figure 6a shows an upper level positive zonal wind anomaly in high latitudes associated with the polar jet. Another extended positive anomaly is observed at subtropical latitudes, with its maximum on the oriental side of the continent and the adjacent Atlantic Ocean. There is also a negative anomaly to the south. They both have values with the same order of magnitude as those observed during $+\sigma$ GF composites. In the lower levels (Fig. 6b) the position of the anticyclone at the southwest side of the South American cone, clearly favors the polar air advection towards the Wet Pampa in Argentina.

All these circulation features will lead to a decrease in surface temperature, which is confirmed by the negative temperature anomalies in the northern part of Argentina (Fig. 7a). The magnitude of these anomalies indicates a considerable decrease in surface temperature over the Wet Pampa region, over an area quite similar to that when there is a GF event. As mentioned before, this situation is caused by an anticyclonic anomaly southwest of the continent at low levels, whose circulation is reinforced by the presence of another anomaly with opposite sign southeast of Argentina (not shown), similar to those observed by Müller et al. (2005) and Müller and Berri (2007). They provide an intense wind anomaly of polar origin which affects the whole troposphere as seen in Fig. 6, and have an impact in the Wet Pampa.

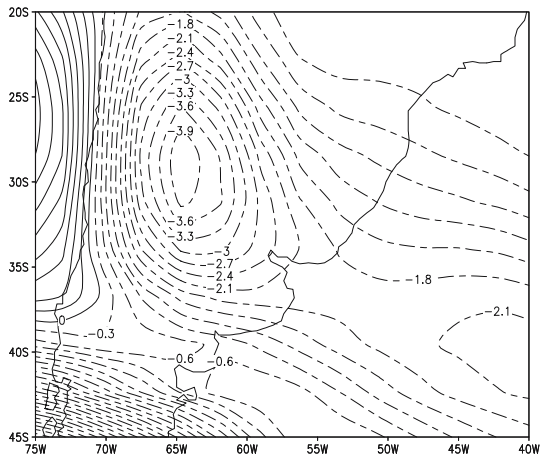

Fig. 7 Surface temperature anomalies (°C) at 850 hPa for day 14 of integration, corresponding to the numerical simulation showed in Fig. 5. Contour interval is 0.3°C

It is important to point out that numerous numeric experiments were performed using different heating sources. For instance, Müller and Ambrizzi (2006) performed simulations positionating forcings according to observed OLR (Outgoing Longwave Radiation) anomalies during the winters with maximum frequency of GF (GF + σ). As one would expect, the forcings can trigger Rossby waves that propagate toward the South American continent creating a circulation pattern favorable for the occurrence of GF events. Nevertheless, extension of the region and the

intensity of the anticyclonic anomalies and cold air advection seem to be not enough to generate a GF event. These results suggest that it is the subtropical and polar waves interaction that creates the right environment for the GF events described in Müller et al. (2005).

3.2.2 *Basic state of minimum GF frequency (–σ)*

Simulations using the $-\sigma$ basic state was also performed in this study. The forcing locations are the same as in the $+\sigma$ basic state i.e., at 40°E, 20°S and 45°E, 40°S. In this basic state, the first forcing is associated with the entrance of the subtropical jet (see Fig. 2b). The second is situated upstream of the region where the zonal wave number $K_s = 0$ (see Fig. 2f) i.e., where the absolute vorticity meridional gradient (β_M) is negative (see Fig. 2d). Therefore, the position of the forcing sources in relation to the mean features of the basic state are similar in both $+\sigma$ and $-\sigma$ cases. Figure 8 shows the meridional wind anomalies at 250 hPa for the day 14 of the integration. Similar to the previous discussion for the $+\sigma$ basic state simulation (Fig. 5a), Rossby wave trains propagates along the subtropical and polar waveguides. In contrast to the K_s field discussed before (Fig. 2e), in this case the waveguide duct is shorter (Fig. 2f). Also, the K_s minimum observed in the midlatitude South America for the $-\sigma$ basic state is displaced southward. In general it can be observed that the trajectory followed by both wave trains in the eastern hemisphere is zonal, but at a certain distance from the source region some curvature appears. This departure from zonality occurs in the western hemisphere at midlatitude over the Pacific Ocean and approximately coincides with regions where K_s is no longer zero (see Fig. 2f). Close to the continent—where there is a minimum in K_s—a divergence in the trajectories of both wavetrains is found. All these features act to avoid a wave interaction over the continent as it is demonstrated by Fig. 8.

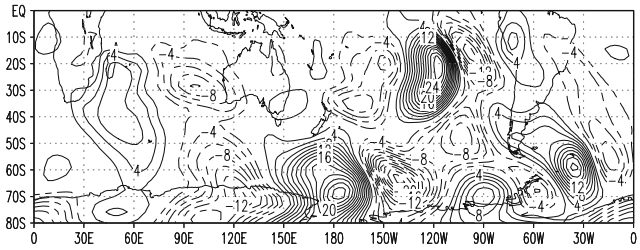

Fig. 8 Meridional wind component anomalies (ms^{-1}) at 250 hPa for day 14 of integration, corresponding to the simulation of $-\sigma$ basic state with two forcings: at 40°E, 20°S and 45°E 40°S. Contour interval is 2 ms^{-1}

Although one can see a negative maximum in the surface temperature anomaly at the northeast of the Wet Pampa (Fig. 9a) the intensity and the position is quite different from that shown in Fig. 7. It is also clear from the wind vector anomalies pattern (Fig. 9b) that the intensity and position of the anticyclone in the southeast Pacific Ocean do not favor frost formation over the region of interest due to the moisture advection from the ocean.

4 A mechanism favoring a higher frequency of GF occurrence

Based on the results of the numerical experiments, in particular for the $+\sigma$ basic state (Sect. 3.1), which showed a

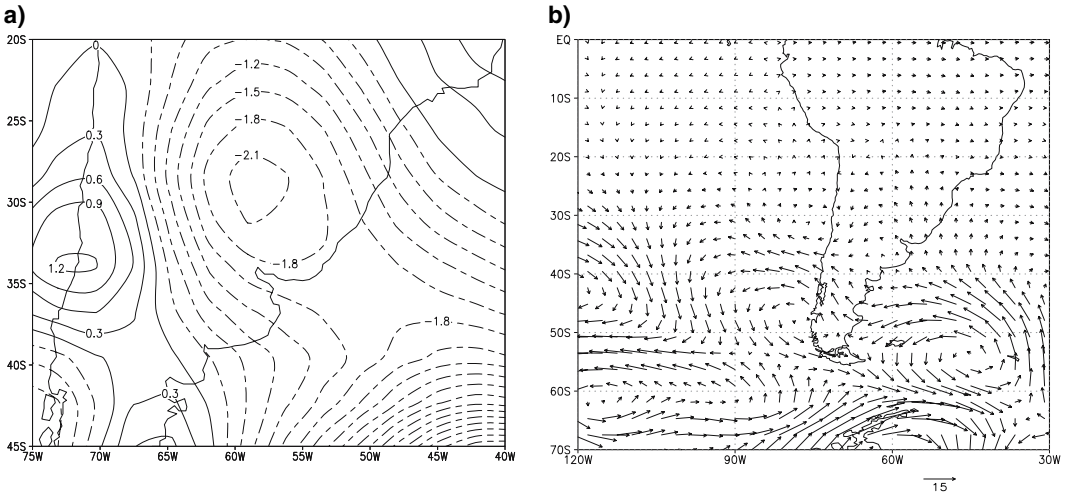

Fig. 9 Surface temperature anomalies (°C) (**a**) and wind vector anomaly at 850 hPa (**b**) for day 14 of integration, corresponding to the numerical simulation depicted in Fig. 8

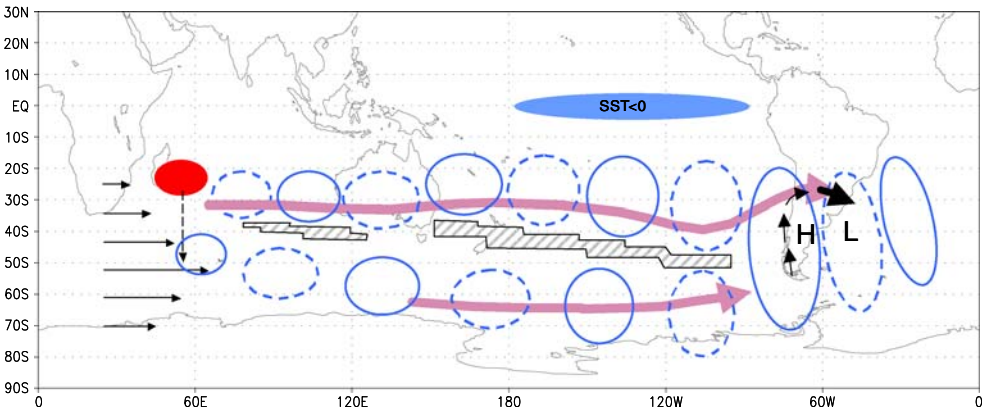

Fig. 10 Conceptual diagram on the physical mechanisms that may favor high frequency occurrence of Generalized Frosts over the Wet Pampa, Argentina (See text for details)

good agreement with the observational analysis done by Müller et al. (2005), a conceptual diagram suggesting a possible physical mechanism to explain the occurrence of GF events over the Wet Pampa is presented in Fig. 10.

The large-scale physical mechanisms associated with GF manifest through teleconnection patterns and are given by stationary Rossby waves. They are generated over the tropical Indian Ocean in a mean flow characterized by a zonal wind meridional gradient (indicated with arrows in Fig. 10). The upper level divergent motion (dashed arrow), probably generated by a tropical source (dark circle), creates perturbations in the subtropics when interfering with the positive meridional gradient of absolute vorticity region that would become a source of Rossby waves. This source region is upstream of the Australian subtropical jet and upstream of the region where the absolute vorticity meridional gradient is negative (stripped area). According to the linear wave theory, this region will reflect the waves, not allowing their propagation through it and therefore a waveguide duct is created to the north and south. In this way, the generated Rossby waves [represented by the sequence of positive (full lines) and negative (dashed lines) meridional wind anomalies zones], propagate along the subtropical and polar waveguides (thick arrows). Close to the South American continent the phases of both wave trains coincide over the region where the propagation inhibition disappears, merging into one single pattern.

The deep ridge in the western part of the continent produces a strong advection by southern winds (thick black arrows), which extends through the whole troposphere before the occurrence of a GF event. Hence, the cold air starts to cross the mountain range first where it is lowest, i.e. in the southern South America, generating anticyclonic vorticity. The advection of this vorticity feeds the continental anticyclone and the maritime cyclone situated downstream. The increase of the pressure gradient over the area leads to a drop in surface temperature in the eastern part of the continent with a strong southern wind component between the high and low pressure systems bringing cold polar air.

The presence of the shaded area in the equatorial eastern Pacific in the Fig. 10 means that negative SST anomalies in this region seems to be important to favor GF events in the Wet Pampa, as indicated by Sea Surface Temperature composite analysis for GF $+\sigma$ of Müller et al. (2005).

5 Conclusions

The observational evidences shown by Müller et al. (2005) and the analysis based on the linear wave theory presented here, allowed the formulation of a hypothesis about how the teleconnection patterns in the Southern Hemisphere are linked to extreme cold events in the Wet Pampa, Argentina. Numerical simulations using a baroclinic model and a basic state formed by the composites of winters with extreme GF frequency were carried out. From the analysis relating observations, theory and modeling, it was possible to formulate a conceptual scheme on the teleconnection mechanisms that act during the austral winters of maximum frequency of GF occurrence.

The linear wave theory offers a simple and useful interpretation of global Rossby wave propagation. According to this theory, the characteristics of the Rossby waves propagation in a given basic state may be determined by the analysis of the K_s parameter. Using this theoretical concept, the distribution of the stationary wave number (K_s) is obtained for austral winters with a maximum ($+\sigma$) and minimum ($-\sigma$) frequency of occurrence of GF in the Wet Pampa. From these fields it is possible to determine the preferential propagation paths of the waves that reach South America. The distribution of K_s emphasizes the important of the jets as efficient wave guides, with a good agreement between their positions and the bands of local K_s maximums, with zonal orientation. Wave numbers 6 and 7 are found along the subtropical jet region in both

basic states analyzed ($+\sigma$ and $-\sigma$) while the wave number 3 dominates in the polar jet region.

For the $+\sigma$ basic state, both the subtropical and polar waveguides are well defined and they show longitudinal extension larger than in the $-\sigma$ case. In fact, it is this difference in the K_s distribution that it may be responsible for the $+\sigma$ and $-\sigma$ occurrence of GF over the Wet Pampa. The position of the waveguides seems to favor the wave interaction observed in the south of South America in the Müller et al. (2005) analysis. Based on the K_s field (Fig. 2e), the trajectory followed by the waves agrees with the theory. It was shown that the separation between the subtropical and polar waveguides occurs just before the south cone of South America. On the other hand, over the continent, around 35°S, 70°W, there is a K_s minimum zone, which forces the waves coming from the subtropical region to turn to the south, meeting the polar waves which are not bound by the waveguide duct anymore. Therefore, this configuration creates the right environment for the wave phase coincidence over the south of South America.

In contrast to the K_s field discussed above, in the case of the $-\sigma$ basic state the waveguide duct is shorter and the waves trapped inside the subtropical and polar waveguides are free to move much earlier than they reach the South American continent. Also, the K_s minimum observed in the subtropical South America for the $+\sigma$ basic state is displaced southward and coincides with the main region of the synoptic systems entrance in the continent. All these features act to avoid a wave interaction over the continent with the waves having their trajectory less zonal than $+\sigma$ case. In this way the cold air irruptions over the Wet Pampa are not favored which agrees with the observed very low frequency of GF.

Through the distribution of K_s and the observational studies of Müller et al. (2005) it was possible to verify the role of atmospheric jets as waveguides and to confirm the importance of Rossby waves in leading to the generation of GF in the Wet Pampa. These results were further checked through numerical simulations using a baroclinic model. From the analysis of the simulated stationary wave patterns it is verified that the principal wave activity takes place inside the subtropical and polar jets that guide the waves in the different basic states studied, though each one has a different propagation pattern. For the $+\sigma$ basic state in particular, two wave trains are well defined: one propagating along the subtropical jet and the other along the polar jet. Their phases coincide before entering the continent as shown by the observations previous to GF events. This configuration establishes an anomalous meridional circulation in the western part of South America. The intense and continuous polar air flux caused by this situation favors the development of the most frequent and/or persistent GF events in the Wet Pampa. The simulations using the $-\sigma$ basic state also show two waves propagating along the subtropical and polar waveguides. However, they do not merge near the west coast of South America, a divergence in the propagation trajectories of the wave trains is observed. In fact, the polar wave crosses the southern tip of the continent, favoring some polar air flux but less intense.

The differences between both basic states are not only verified in the trajectories followed by the waves, but also in the phase and amplitude they have when reaching the South American continent. For example for $+\sigma$, the amplitude of the upper levels meridional wind anomalies (in agreement with observations) is twice of that found in the numerical experiments for $-\sigma$ basic state. At low levels, the wind field also reflects disparities between the two basic states, in spite of some similarity in the stimulated negative anomalie of surface temperature. However, a temperature drop that can cause frosts in the Wet Pampa is only possible during the $+\sigma$ configuration. In this case the circulation at low levels is from the south to southwest, while in $-\sigma$ the dominant component is in the east sector. In the first case the Wet Pampa region will be under adequate conditions to generate frosts, particularly of advective type due to the entrance of cold dry air over the region; whereas that region in $-\sigma$ basic state is under the influence of humid air advection which does not favor frosts.

Acknowledgments We are grateful to Dr George Kiladis and to an anonymous reviewer for their suggestions, which contributed to improve this work. GM is also grateful for the CNPq grant no. 152039/2004-0. TA had also partial support from CNPq, FAPESP and IAI-CRN055. This paper is part of the first author's PhD Thesis at the University of Buenos Aires.

References

Ambrizzi T, Hoskins BJ (1997) Stationary Rossby wave propagation in a baroclinic atmosphere. Q J R Meteorol Soc 123:919–928

Ambrizzi T, Hoskins BJ, Hsu HH (1995) Rossby wave propagation and teleconnection patterns in the austral winter. J Atmos Sci 52:3661–3672

Berbery EH, Nogués-Paegle J, Horel JD (1992) Wavelike Southern Hemisphere extratropical teleconnections. J Atmos Sci 49:155–177

Berbery EH, Vera CS (1996) Characteristics of the Southern hemisphere winter storm track with filtered and unfiltered data. J Atmos Sci 53:468-481

Cavalcanti I (2000) Teleconnection patterns orographically induced in model results and from observational data in the austral winter of the Southern Hemisphere. Int J Climatol 20:1191–1206

Cavalcanti I, Kayano MT (1999) High frequency patterns of the atmospheric circulation over the Southern Hemisphere and South American. Meteorol Atmos Phys 69:179–193

Garreaud RD (2000) Cold air incursions over subtropical South America: mean structure and dynamics. Mon Wea Rev 128:2544–2559

Hoskins BJ (1983) Dynamical processes in the atmosphere and the use of models. Q J R Meteorol Soc 109:1–21

Hoskins BJ, Ambrizzi T (1993) Rossby wave propagation on a realistic longitudinally varying flow. J Atmos Sci 50:1661–1671

Hoskins BJ, Karoly DJ (1981) The steady linear responses of a spherical atmosphere to thermal and orographic forcing. J Atmos Sci 38:1179–1196

Hoskins BJ, Simmons AJ (1975) A multi-layer spectral model and the semi-implicit method. Q J R Meteorol Soc 101:637–655

Jin FF, Hoskins BJ (1995) The direct response to tropical heating in a baroclinic atmosphere. J Atmos Sci 52:307–319

Karoly DJ (1983) Rossby wave propagation in a barotropic atmosphere. Dyn Atmos Oceans 7:111–125

Kiladis GN (1998) Observations of Rossby waves linked to convection over the eastern tropical Pacific. J Atmos Sci 55:321–339

Marengo JA, Cornejo A, Satyamurty P, Nobre C, Sea W (1997) Cold surges in tropical and extratropical South America: the strong event in June 1994. Mon Wea Rev 125:2759–2786

Marengo JA, Ambrizzi T, Kiladis G, Liebmann B (2002) Upper-air wave trains over the Pacific Ocean and wintertime cold surges in tropical-subtropical South America leading to freezes in Southern and Southeastern Brazil. Theor Appl Climate 74:243–247

Müller GV (2006) Variabilidad Interanual de las Heladas en la Pampa Húmeda. Braz J Meteorol 21:135–141

Müller GV, Ambrizzi T (2006) Teleconnection patterns associated with extreme frequency of Generalized Frosts. Part II: Origin and evolution of the Rossby waves propagation patterns in the Austral Hemisphere'. In: 8th International conference on southern hemisphere meteorology and oceanography. Foz do Iguazu, Brasil

Müller GV, Berri GJ (2007) Atmospheric circulation associated with persistent generalized frosts in central-southern South America. Mon Wea Rev 135(4):1268–1289

Müller GV, Nuñez MN, Seluchi ME (2000) Relationship between ENSO cycles and frosts events within the Pampa Húmeda region. Int J Climatol 20:1619–1637

Müller GV, Ambrizzi T, Núñez MN (2005) Mean atmospheric circulation leading to generalized frosts in Central Southern South America. Theor Appl Climate 82:95–112

Seluchi ME, Marengo JA (2000) Tropical-midlatitude exchange of air masses during summer and winter in South America: climatic aspects and examples of intense events. Int J Climatol 20:1167–1190

Valdes PJ, Hoskins BJ (1989) Linear stationary wave simulations of the time-mean climatological flow. J Atmos Sci 46:2509–2527

Vera CS, Vigliarolo PK (2000) A diagnostic study of cold-air outbreaks over South America. Mon Wea Rev 128:3–24

Yang GY, Hoskins BJ (1996) Propagation of Rossby waves of nonzero frequency. J Atmos Sci 53:2365–2378